ACS Energy LETTERS

http://pubs.acs.org/journal/aelccp

PERSPECTIVE

Electro- and Photoreduction of Carbon Dioxide: The Twain Shall Meet at Copper Oxide/Copper Interfaces

C. Janaky,[†,‡] D. Hursán,[†,‡] B. Endrődi,[†,‡] W. Chanmanee,[⊥] D. Roy,[§] D. Liu,[§] N. R. de Tacconi,[§] B. H. Dennis,[⊥] and K. Rajeshwar*[,§]

[†]MTA-SZTE, Lendület Photoelectrochemistry Research Group and [‡]Department of Physical Chemistry and Materials Science, University of Szeged, Rerrich Square 1, Szeged H-6720, Hungary

[§]Department of Chemistry and Biochemistry and [⊥]Department of Mechanical and Aerospace Engineering, University of Texas at Arlington, Arlington, Texas 76019, United States

ABSTRACT: **Of the myriad electrode materials that have been used for electrochemical (EC) and photoelectrochemical (PEC) reduction of carbon dioxide in aqueous media, copper oxide/copper interfaces have shown a remarkable range of hydrocarbon and oxygenated products including acids, aldehydes, ketones, and alcohols. This Perspective highlights experimental evidence for the fact that both EC and PEC reduction scenarios have similar chemical and morphological underpinnings in the in situ formation of copper nano- or microcubes on the (photo)cathode surface. Recent rapid developments in our fundamental understanding of these interfaces and areas requiring further studies are discussed in light of recent studies in the authors' laboratories and elsewhere.**

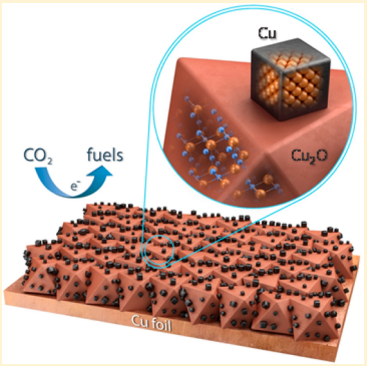

Much has been written already about the technological relevance of carbon dioxide (CO_2) conversion and utilization.[1−3] Whether it makes sense from an overall energy balance and practical feasibility perspective, it is hardly debatable that electrochemical (EC) reduction and subsequent hydrogenation/oxygenation of an inert molecule such as CO_2 has considerable fundamental appeal. On the other hand, the energy input needed for the process is considerably ameliorated by the addition of solar excitation of the active material (a photoresponsive semiconductor) such that the CO_2 reduction now occurs at 700 mV positive of the thermodynamic threshold. Both process variants are hardly new, and the electroreduction concept was first published some 150 years ago.[4] The modern era of CO_2 electroreduction, however, can be traced back to the 1970s and 1980s. The photoelectrochemical (PEC) approach first surfaced around the same time, with the seminal paper appearing in 1978.[5] Since then, interest in both the EC and PEC approaches has been frenetic, especially during the past 5 years

The one-electron reduction of CO_2 to the radical anion is a high-energy pathway and occurs at a standard potential of −1.90 V in water.[6] On the other hand, the two-electron reduction generates CO via a pathway that is shared by enzymatic processes and metal electrode surfaces. Subsequent conversion to hydrocarbons and oxygenates, however, requires the use of a catalyst and cogeneration of hydrogen. A wide range of electrode materials and electrolytes have been deployed for the EC and PEC conversion of CO_2; many reviews and book chapters exist.[6−13] In terms of sustainability and process scalability, however, only a limited range of candidates are worthy of serious consideration for technological deployment. Thus, the use of earth-abundant and nontoxic electrode materials has considerable appeal relative to noble metals (e.g., Pt, Ru, Rh, etc.) or nonabundant elements (e.g., Ga, In, etc.). Likewise, notwithstanding the limited solubility of CO_2 in water (0.033 M at 298 K and 1 atm), the use of aqueous electrolytes presents considerable practical advantages relative to aprotic solvents and ionic liquids. Approaches involving semiconductor suspensions and sacrificial reagents (the so-called "photocatalytic" (PC) processes),[14,15] while extremely simple and attractive from an initial materials screening perspective, will not be practical. For example, (a) the products are cogenerated in close proximity in PC reactors rather than in separate compartments as in the EC and PEC counterparts, (b) recovery and reuse of the photocatalyst necessitates an additional step in PC reactors, and (c) back-reactions are especially prevalent and the system attains a photostationary state. This Perspective thus focuses on the EC/PEC process

Received: April 20, 2016
Accepted: May 11, 2016

DOI: 10.1021/acsenergylett.6b00078
ACS Energy Lett. XXXX, XXX, XXX−XXX

variant involving one such intriguing electrode material, namely, copper oxide decorated with copper nano- or micrometer-sized particles. This rather complex electrode material henceforth is simply designated as Cu_xO/Cu.

Peculiar Case of Copper Oxide/Nanoparticulate Copper. Of all the myriad metals that have been used for EC reduction of CO_2, only copper has shown a proclivity to generate C1−C3 hydrocarbons and oxygenated products. Copper oxide is a semiconductor, and both Cu_2O and CuO are known to exhibit p-type semiconductor behavior. The so-called "oxide-derived" Cu[16,17] has been shown to have much higher selectivity toward CO_2 electroreduction (relative to the hydrogen evolution reaction or HER) than does polycrystalline copper. Thus, the Cu_xO/Cu interface is unusual in that it can be deployed for both EC and PEC reduction of CO_2. Finally, while demand for copper metal generally has soared because of power transmission and microelectronics industry needs, it still is an earth-abundant and nontoxic material. For all of these reasons, the liquid junction formed by this composite interface forms the focus of this Perspective.

> Of all the myriad metals that have been used for EC reduction of CO_2, only copper has shown a proclivity to generate C1−C3 hydrocarbons and oxygenated products.

Interest in Cu_2O first began in the 1920s, and subsequently both oxides of copper were evaluated for use in solid-state photovoltaic devices.[18] The earliest report on the use of these metal oxides in PEC devices dates back to the 1970s.[19] The first report of the use of hydrous Cu_2O suspensions for CO_2 photoreduction occurred much later in 1989.[20] The use of Cu_2O photocathodes began soon thereafter, and there has been explosive growth of interest in this PEC approach, particularly since ∼2010. The various aspects of the preparation, characterization, and use of Cu_2O have been reviewed.[18]

The oxide layers are generally grown by thermal annealing of polycrystalline copper foils in air. Both the annealing time and annealing temperature are crucial variables in dictating the subsequent behavior of the oxides, as discussed later. Thermal growth of copper oxide nanowires on copper foil has been reviewed.[21] Electrosynthesis is another powerful tool for preparing Cu_xO layers or nanoparticles;[22−24] modifications in deposition bath can be used to tune the nanoparticle morphology, as demonstrated in these studies. This aspect is further addressed below within the context of product selectivity in CO_2 reduction.

Both Oxide Phases Are Important in the PEC Activity for CO_2 Reduction. Thermal annealing of a copper foil generates both copper oxides (i.e., Cu_2O and CuO), whose relative dominance can be tracked by X-ray powder diffraction (XRD). As shown in Figure 1a, high aspect ratio (>200), dense, vertically standing copper oxide heterojunction nanowires were fabricated by simply heating a copper substrate in air. Interestingly, the PEC activity for CO_2 reduction for these fabricated materials appears to be closely correlated with the relative dominance of the two formed phases, Cu_2O and CuO, as established by quantitative analyses of XRD data (Figure 1b,c). The sample with the more dominant Cu_2O phase (500 °C, Figure 1b; 4 h, Figure 1c) was seen to afford the highest photocurrent for CO_2 reduction.

> Thermal annealing of a copper foil generates both copper oxides (i.e., Cu_2O and CuO), whose relative dominance can be tracked by X-ray powder diffraction (XRD).

In Situ Formation of Copper on Cuprous Oxide Photocathodes and Consequences in Terms of PEC Activity. On the notion that copper that is formed in situ on the Cu_2O surface during photoirradiation in CO_2-containing solutions plays a key role in the PEC activity, the following series of comparative experiments were performed. The Cu_2O films were electrodeposited on Cu foils and glassy carbon electrodes[24] and irradiated with simulated sunlight for different time periods (5, 10, 30, 60 min) in 0.1 M $NaHCO_3$/satd. CO_2 solution (to mimic the conditions in CO_2 photoelectrolysis). No external bias potential was applied to the photocathode in these experiments. As a control measurement, an identical Cu_2O film was electroreduced (for 60 min) at $E = -1.5$ V (vs Ag/AgCl reference) to obtain Cu_2O-derived metallic copper. The first striking difference was the color of the samples (Figure 2), namely, the oxide film became progressively darker with increasing irradiation time (in fact, the sample irradiated for 60 min was completely black). XRD patterns were recorded to prove that this change in the color was coupled with the increasing Cu content of the samples (note that no CuO was detected). Rietveld refinement of the XRD patterns proved that the Cu_2O/Cu ratio systematically increased in the series of samples and it reached 4:1 after 60 min of irradiation.

Scanning electron microscopy (SEM) images (Figure 3) were taken to study the morphological changes associated with Cu formation in the samples. While the bare Cu_2O layer showed the characteristic nanocrystal morphology (Figure 3a),[24] important changes were observed even after only 5 min of irradiation. In this case, the initial crystallites could still be seen, but they lost their sharp edges, and Cu nanocubes (50−80 nm) were formed on the surface. When continuing the irradiation, the initial morphology changed and a porous Cu film was obtained (Figure 3b). The morphology of an *electro*reduced Cu oxide sample was also studied for comparison (Figure 3c). A relatively compact structure was found in this case, where the surface was decorated with small-sized (∼20 nm) nanocubes. Note that this morphology is rather similar to the one shown for the Cu_2O sample irradiated for short timeframes (Figure 3b), although the nanoparticle size was distinctly smaller for the electroreduced sample. Irradiation for longer times (e.g., 60 min, Figure 3d) resulted in markedly altered morphology from that in panel (b), reflecting further chemical changes of the oxide layer. This corresponds to the blackened layer visually seen in Figure 2.

The distinct morphological differences highlighted above are also reflected in the electrocatalytic properties of the samples. The first striking variance is manifested in the electroactive surface area (as deduced from cyclic voltammetry, Figure 4). While the electroreduced samples had 3−4 times higher surface roughness compared with the flat Cu electrode, the same ratio was around 6−7 for the photoreduced sample (Figure 4a). Subsequently, linear sweep voltammograms were recorded in HCO_3^-/CO_2 solution to assess the electrocatalytic activity of the samples. The most important observation was the shift in

DOI: 10.1021/acsenergylett.6b00078
ACS Energy Lett. XXXX, XXX, XXX−XXX

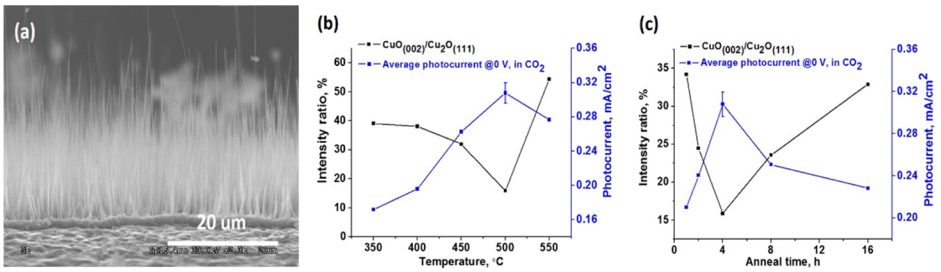

Figure 1. Side view (a) SEM images of copper-supported oxide layers grown by thermal annealing at 500 °C for 4 h. Panels b and c map the correlation between the relative fraction of CuO and Cu_2O (as established by powder XRD analyses) and the average photocurrent for CO_2 reduction as a function of thermal annealing temperature (at a fixed 4 h time) (b) and time (at fixed 500 °C anneal temperature) (c). The photocurrents were measured in CO_2-saturated 0.1 M sodium sulfate at zero applied bias (i.e., at short-circuit). The error bars in (b) and (c) were obtained from measurements on eight separate samples.

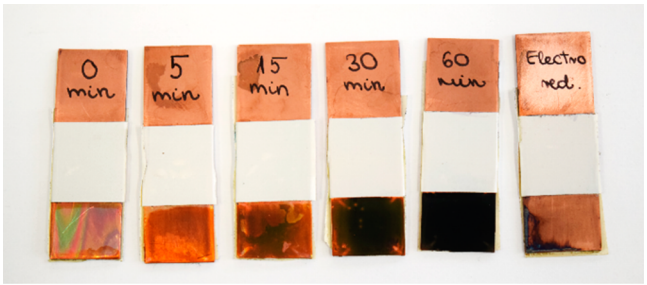

Figure 2. Photographs of slides containing Cu_2O layers irradiated in CO_2-containing solutions for varying times without an externally applied bias potential. An electroreduced control sample (refer to the text) is also shown for comparison.

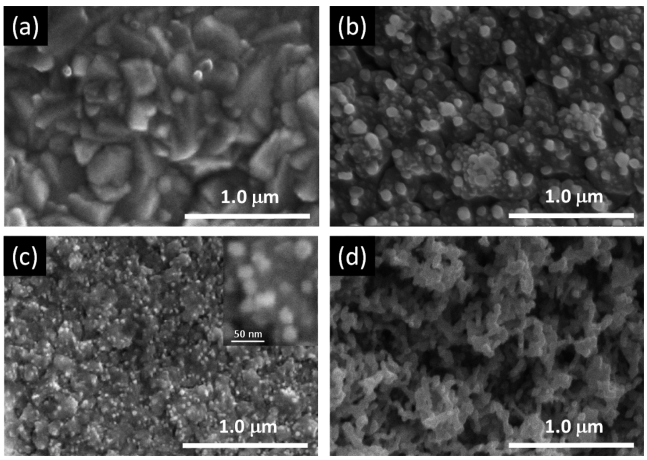

Figure 3. SEM images of the various Cu_2O-derived films. (a) Bare Cu_2O, (b) Cu_2O irradiated with simulated sunlight for 15 min, (c) Cu_2O electroreduced at −1.5 V (vs Ag/AgCl/3 M NaCl) for 60 min, and (d) Cu_2O irradiated with simulated sunlight for 60 min.

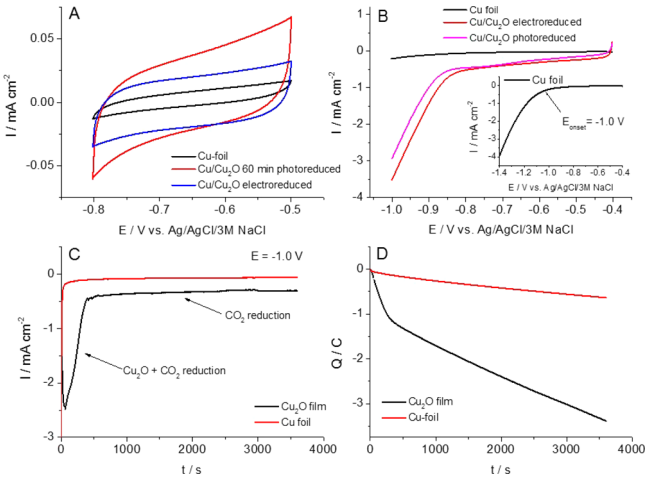

Figure 4. (a) Cyclic voltammograms of the different Cu_2O-derived films, registered in 0.1 phosphate buffer solution (pH = 7) at a sweep rate of 25 mV s^{-1}. (b) Linear sweep voltammetry curves recorded for the different Cu_2O-derived films in 0.1 M $NaHCO_3$/satd. CO_2 solution at a sweep rate of 25 mV s^{-1}. (c,d) Current−time and charge−time curves registered for a Cu foil and Cu_2O film in 0.1 $NaHCO_3$/satd. CO_2 solution at E = −1.0 V potential (vs Ag/AgCl reference).

the onset potential. While for the bulk Cu foil CO_2 reduction started at E = −1.0 V (vs Ag/AgCl reference), the onset potential was notably more positive for the Cu_2O-derived Cu samples (−0.85 and −0.90 V for the electroreduced and photoreduced samples, respectively; Figure 4b).

This latter observation is consistent with literature data where a 150−200 mV shift was seen in the onset potential when comparing bulk and oxide-derived Cu.[16] To prove that these increased currents were related to CO_2 reduction, and not to the reduction of Cu_2O traces present in the samples, long-term electrolysis was also performed on both Cu_2O and Cu electrodes (Figure 4c,d). While at the initial stage of the electrolysis the reduction of Cu_2O and CO_2 occurred in parallel, after the oxide was completely reduced (note that the necessary charge perfectly matches the stoichiometric amount, 1 C), CO_2 reduction was sustained on the oxide-derived metal surface. Thus, the difference between the two samples cannot be simply ascribed to the difference in surface area; rather, other structural factors (nanoparticle size, crystal facets, interparticle grain boundaries, etc.) also must contribute to the enhanced activity (see below).

The gradual conversion of Cu_xO to metallic copper during the PEC processes has at least two effects on PEC performance. First, the formation of traces of Cu (cf. Figure 3b) enhances the PEC activity due to the intrinsic catalytic activity of the Cu nanocubes. Existence of a Schottky junction between Cu_2O and Cu can also facilitate e^-/h^+ separation, thus enhancing the catalytic activity. On the other hand, especially after longer irradiation, gradual consumption of the Cu_xO semiconductor component (because of photocorrosion) leads to a decrease in light absorption and consequently results in the cessation of PEC activity. Note, however, that the photoreduction studies

DOI: 10.1021/acsenergylett.6b00078
ACS Energy Lett. XXXX, XXX, XXX−XXX

presented here were performed in the absence of any external bias potential.

The photocorrosion of Cu_xO in this system is not a fatal flaw because the electrode material can be regenerated, as demonstrated by our recent study on Cu_2O/CNT photoelectrodes.[24] Electro-oxidation of the photogenerated Cu (to Cu_2O) occurred during the dark periods periodically inserted into the photoelectrolysis protocol. It is worth noting that this EC self-healing was enabled by selection of an optimal potential after careful analysis of the Pourbaix diagram for Cu.

Reduction Products, Causal Factors in Product Distribution, and Crystal Engineering. The Cu_xO/Cu interface is remarkable in the range of products that have been reported from EC and PEC reduction of CO_2. Table 1 collates the various reduction steps possible and corresponding redox potentials. Discounting the one-electron radical pathway, anywhere from 2 electrons up to 18 electrons can be delivered to the CO_2 molecule (Table 1). Clearly, carbon−carbon bond formation upon deeper reduction is predicated upon initial binding of intermediates such as CO at active sites on the solid surface. It is hardly surprising that the surface morphology plays a key role in product selectivity. While many mechanistic details still remain to be elucidated, high-energy steps and edges on the crystal surface are currently believed to stabilize and afford the chemisorbed C1 and C2 intermediates to undergo intermolecular C−C coupling.

The Cu_xO/Cu interface is remarkable in the range of products that have been reported from EC and PEC reduction of CO_2.

As many as 16 reaction products were observed in one EC reduction study on Cu, and of these, 12 were C2 or C3 species, comprised of a range of oxygenated species including hydrocarbons, ketones, aldehydes, carboxylic acids, and alcohols.[25] In our own PEC reduction studies on hybrid CuO/Cu_2O photocathodes, clean conversion of CO_2 exclusively to methanol was initially observed.[26,27] However, our two later studies involving a different set of experimental conditions also revealed the additional formation of ethanol and isopropanol[28] and ethanol, formaldehyde, acetaldehyde, and acetone[29] in addition to methanol.

Theoretical insights[30,31] considerably aid in guiding experimentation and also for rationalizing the experimentally observed product selectivity trends. Thus, analysis of trends in the binding energies for the CO_2 reduction intermediates revealed the protonation of adsorbed CO as the most important step in dictating the overpotential magnitude.[31] Density functional theory (DFT) calculations have also been presented to this end.[30]

Ethylene and ethanol have higher energy densities and commercial value than the C1 counterparts. Thus, much effort has focused on optimizing, for example, the C_2H_4/CH_4 product ratio in EC reduction schemes. In this vein, copper microcubes containing a large number of exposed (100) facets (see Figure 5) have shown a much higher ratio than unstructured polycrystalline copper.[32−36] Their manifestation in PEC reduction was addressed above (cf. Figure 4b). While this morphology is derived from the use of copper(I) halides

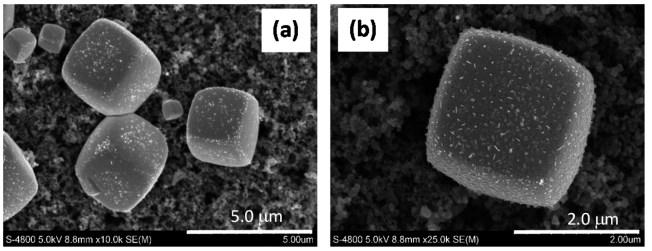

Figure 5. Representative SEM images at two magnifications of a Cu_xO/Cu microcube layer electrodeposited on a gas diffusion electrode (GDE) at −0.4 V (60 °C) from a pH 7 solution of 0.2 M $CuSO_4$ + 0.1 M CuBr + 2 M lactic acid.

Table 1. Nonradical Reduction Pathways for Carbon Dioxide

product	reaction	standard reduction potential (V vs SHE, the behavior of copper-based electrodes calls into question, our traditional notion of a chemical catalyst as an agent that does not itself undergo chemical change!at pH = 7)
carbon monoxide	$CO_2 + 2H^+ + 2e^- = CO + H_2O$	−0.51
	Hydrocarbons	
methane	$CO_2 + 8H^+ + 8e^- = CH_4 + 2H_2O$	−0.24
ethane	$2CO_2 + 14H^+ + 14e^- = C_2H_6 + 4H_2O$	−0.27
ethylene	$2CO_2 + 12H^+ + 12e^- = C_2H_4 + 4H_2O$	−0.34
	Oxygenates	
formic acid	$CO_2 + 2H^+ + 2e^- = HCOOH$	−0.58
oxalic acid	$2CO_2 + 2H^+ + 2e^- = (COOH)_2$	−0.87
formaldehyde	$CO_2 + 4H^+ + 4e^- = HCHO + H_2O$	−0.48
methanol	$CO_2 + 6H^+ + 6e^- = CH_3OH + H_2O$	−0.39
ethanol	$2CO_2 + 12H^+ + 12e^- = C_2H_5OH + 3H_2O$	−0.33
propanol	$3CO_2 + 18H^+ + 18e^- = C_3H_7OH + 5H_2O$	−0.32

DOI: 10.1021/acsenergylett.6b00078
ACS Energy Lett. XXXX, XXX, XXX−XXX

(chloride and bromide) as precursors (cf. Figure 5), in situ X-ray absorption spectroscopy (XAS) has revealed that copper(I) oxide, formed by the initial hydrolysis of the halide, is really the precursor to copper nanocube formation.[35] Undoubtedly, the deployment of new in situ probes such as XAS along with online mass spectrometry and techniques such as nuclear magnetic resonance (NMR) spectroscopy should continue to provide insights into deposition mechanisms and reaction pathways. Careful isotope labeling studies will also contribute to further mechanistic insights.

The electrolytes used, the potentials applied, and the crystal topology all have a major influence on EC reduction and, by extension, the PEC reduction product selectivity. The oxide layer thickness on copper is another crucial factor as is the local pH at the oxide/copper/electrolyte interface. A high local pH, for example, could suppress the HER and promote C2 coupling.[36] Finally, "crystal engineering" could be used to tune product selectivity. Two examples of this may be cited. Controlled chemical etching has been demonstrated[37] as a strategy for exposing high-energy (110) facets on copper nanocubes; the resultant EC reduction activity was significantly enhanced. The grain boundary density has been shown to be correlated to CO reduction activity for oxide-derived metals, suggesting another route for externally manipulating the catalytic activity of the surface.[38]

Electrode and Reactor Designs for EC and PEC Reduction of CO_2. The vast majority of the initial studies were confined to stationary laboratory-scale batch reactors in both cases. Electrode designs also come into play. For example, a porous hollow fiber copper electrode with a compact three-electrode geometry has been shown to provide a large-area three-phase boundary for CO_2 EC reduction.[39] Borrowing from the fuel cell playbook, a GDE provides for operation at pressures higher than the ambient.[9] Solid-oxide fuel cells also provide for a matrix for performing CO_2 electrolysis at higher temperatures with concomitant improvements in process thermodynamics and kinetics.[9] Energy efficiencies for various CO_2 electrolyzer designs have been compared.[3] The challenge here is to simultaneously secure high values of energy efficiency and cathodic current density. Reactor designs for PEC reduction of CO_2 have been reviewed.[13] In our own studies of a continuous-flow PEC reactor (CFPR) for CO_2 reduction, interesting shifts in product distribution away from C1 (methanol) to longer chain products were observed because of the small volume in the cathode microchannel and consequential ease of coupling of the initial electrogenerated precursors.[28]

Future Outlook. In summary, this Perspective has highlighted the important fact that morphological evolution of the (photo)cathode during the complex steps involved in the addition of electrons and protons to CO_2 has similar underpinnings in both EC and PEC reduction scenarios. Nonetheless and as pointed out earlier, the chemical changes undergone by the copper oxide surface during CO_2 (photo)-reduction need not be considered a fatal flaw in the use of this intriguing material. Many natural assemblies (e.g., the plant photosynthesis apparatus) do indeed undergo self-repair mechanisms after exposure to high photon fluxes. In a similar fashion, a periodic reactivation step to regenerate CO_2 reduction activity may be built into the overall process design to combat too deep of a reduction of the copper oxide layer.

Interestingly, however, the behavior of copper-based electrodes calls into question our traditional notion of a chemical catalyst as an agent that does not itself undergo chemical change! This aspect certainly is not the only puzzle that the Cu_xO/Cu/liquid interface holds; many more surprises undoubtedly await the intense EC and PEC scrutiny of it in the coming months and years. Finally, the features of copper oxide/copper interfaces as noted here may not be unique; recent studies highlighting similar trends in other metal oxide/metal interfaces, including Au, Sn, and even Co, are worthy of note.[40−42]

The behavior of copper-based electrodes calls into question our traditional notion of a chemical catalyst as an agent that does not itself undergo chemical change!

Finally, notwithstanding the remarkable strides that have been made in the past 5 years in our understanding of copper-based electrodes and photoelectrodes for CO_2 (photo)-reduction, the product fluxes need to be boosted significantly to levels that are sufficiently high for reactor scale-up and engineering. There are promising avenues, including the incorporation of additional metal ions into the copper oxide host framework (e.g., $CuFeO_2$ and $CuNb_2O_6$)[43,44] or the use of 3D electrode architectures of highly conductive nanocarbons such as aligned carbon nanotubes or graphene foams. Finally, further advances in electrode and reactor designs also have to occur to translate the laboratory-scale findings to technological readiness.

AUTHOR INFORMATION

Corresponding Author

*E-mail: rajeshwar@uta.edu.

Notes

The authors declare no competing financial interest.

Biographies

Csaba Janáky obtained his Ph.D. at the University of Szeged in 2011. Subsequently, he was a Marie Curie Fellow at the University of Texas at Arlington between 2011 and 2013. Since 2014, he has been the Principal Investigator of the MTA-SZTE "Momentum" Photoelectrochemistry Research Group, supported by the excellence program of the Hungarian Academy of Sciences. His scientific interests include various aspects of energy-oriented semiconductor electrochemistry and photoelectrochemistry.

Dorottya Hursán is a Ph.D. student at the University of Szeged, under the supervision of Prof. Janáky. Her research focuses on the electrochemical and photoelectrochemical conversion of CO_2.

Balázs Endrődi completed his education at the University of Szeged, where he obtained his Ph.D. in 2015. Currently he is an assistant professor at his alma mater, focusing on electrochemical energy conversion.

Wilaiwan Chanmanee received her M.Sc. degree in Environmental Engineering at Kasetsart University (Thailand) in 2005 and went on to receive her Ph.D. degree in Environmental Science at Chulalongkorn University (Thailand) in 2008. She is a postdoctoral researcher at the Center for Renewable Energy and Science Technology at the University of Texas at Arlington.

Daipayan Roy, a native of India, is currently a first-year graduate student at the University of Texas, Arlington. He completed his

DOI: 10.1021/acsenergylett.6b00078
ACS Energy Lett. XXXX, XXX, XXX−XXX

Master's degree from the University of Pune with a specialization in inorganic chemistry in 2015.

Dong Liu received his Ph.D. in Materials Science and Engineering from the University of Texas at Arlington in 2015. He is a postdoctoral researcher at the Center for Renewable Energy and Science Technology at the University of Texas at Arlington.

Norma R. de Tacconi received her Ph.D. in Electrochemistry (1975) from the University of La Plata and INIFTA, Argentina. After postdoctoral research (1977−1978) at the University of Paris VII, France, she was scientist of INIFTA/CONICET until 1991 when she moved to the United States. She is a Research Associate Professor at the University of Texas at Arlington, and her current research interests are on metal and semiconductor nanostructures and nanocomposites for (photo)electroreduction of carbon dioxide.

Brian H. Dennis received his Ph.D. in Aerospace Engineering (2000) from the Pennsylvania State University where he focused on the development of numerical methods for simulating the interaction of conducting fluids with electromagnetic fields. He is currently a Professor of Mechanical & Aerospace Engineering at the University of Texas at Arlington. His current research interests are on the design, numerical simulation, and fabrication of electrochemical and photoelectrochemical reactors.

Krishnan Rajeshwar completed his Masters and Ph.D. degrees in solid-state chemistry at the Indian Institute of Technology (Kharagpur, India) and Indian Institute of Science (Bengaluru, India), respectively. After postdoctoral training at Colorado State University (Fort Collins, CO) in the area of energy R&D, he joined the faculty of the University of Texas at Arlington in 1983, where he is currently Distinguished University Professor. He is also Senior Vice President and President-Elect of the Electrochemical Society. His research interests span a broad spectrum in materials chemistry and design for thermal, electrochemical, and photoelectrochemical energy conversion.

■ ACKNOWLEDGMENTS

We thank the following agencies for partial funding support of the research described herein: the National Science Foundation (CHE-1303803) (to K.R.); Hungarian Academy of Science, "Momentum" Excellence Program (LP2014-3) (to C.J.); and NASA (Award No. NNL15AA08C to K.R., N.d.T., and B.H.D.). The authors also thank Rendernet Ltd. for assistance in preparing the artwork in the TOC. The constructive criticisms provided by three anonymous reviewers on an initial version of this manuscript are much appreciated.

■ REFERENCES

(1) Olah, G. A.; Prakash, G. K. S.; Goeppert, A. Anthropogenic Chemical Carbon Cycle for a Sustainable Future. *J. Am. Chem. Soc.* **2011**, *133*, 12881−12898.

(2) Oloman, C.; Li, H. Electrochemical Processing of Carbon Dioxide. *ChemSusChem* **2008**, *1*, 385−391.

(3) Whipple, D. T.; Kenis, P. J. A. Prospects of CO_2 Utilization via Direct Heterogeneous Electrochemical Reduction. *J. Phys. Chem. Lett.* **2010**, *1*, 3451−3458.

(4) Royer, M. E. Réduction de L'acide Carbonique En Acide Formique. *C. R. Hebd. Séanc. Acad. Sci., Paris* **1870**, *70*, 731−732.

(5) Halmann, M. Photoelectrochemical Reduction of Aqueous Carbon Dioxide on p-Type Gallium Phosphide in Liquid Junction Solar Cells. *Nature* **1978**, *275*, 115−116.

(6) Costentin, C.; Robert, M.; Savéant, J.-M. Catalysis of the Electrochemical Reduction of Carbon Dioxide. *Chem. Soc. Rev.* **2013**, *42*, 2423−2436.

(7) Hori, Y. Electrochemical CO_2 Reduction on Metal Electrodes. In *Modern Aspects of Electrochemistry*; Vayenas, C. G., White, R. E., Gamboa-Aldeco, M. E., Eds.; Springer, 2008; pp 89−189.

(8) Roy, S. C.; Varghese, O. K.; Paulose, M.; Grimes, C. A. Toward Solar Fuels: Photocatalytic Hydrocarbons. *ACS Nano* **2010**, *4*, 1259−1278.

(9) Kondratenko, E. V.; Mul, G.; Baltrusaitis, J.; Larrazabal, G. O.; Perez-Ramirez, J.; Larrazábal, G. O.; Pérez-Ramírez, J. Status and Perspectives of CO_2 Conversion into Fuels and Chemicals by Catalytic, Photocatalytic and Electrocatalytic Processes. *Energy Environ. Sci.* **2013**, *6*, 3112−3135.

(10) Ogura, K. Electrochemical Reduction of Carbon Dioxide to Ethylene: Mechanistic Approach. *Journal of CO2 Utilization* **2013**, *1*, 43−49.

(11) Lu, Q.; Rosen, J.; Jiao, F. Nanostructured Metallic Electrocatalysts for Carbon Dioxide Reduction. *ChemCatChem* **2015**, *7*, 38−47.

(12) Chang, X.; Wang, T.; Gong, J. CO_2 Photo-Reduction: Insights into CO_2 Activation and Reaction on Surfaces of Photocatalysts. *Energy Environ. Sci.* **2016**, DOI: 10.1039/C6EE00383D.

(13) Li, K.; An, X.; Park, K. H.; Khraisheh, M.; Tang, J. A Critical Review of CO_2 Photoconversion: Catalysts and Reactors. *Catal. Today* **2014**, *224*, 3−12.

(14) Rajeshwar, K.; Thomas, A.; Janaky, C. Photocatalytic Activity of Inorganic Semiconductor Surfaces: Myths, Hype, and Reality. *J. Phys. Chem. Lett.* **2015**, *6*, 139−147.

(15) Inoue, T.; Fujishima, A.; Konishi, S.; Honda, K. Photoelectrocatalytic Reduction of Carbon Dioxide in Aqueous Suspensions of Semiconductor Powders. *Nature* **1979**, *277*, 637−638.

(16) Li, C. W.; Kanan, M. W. CO_2 Reduction at Low Overpotential on Cu Electrodes Resulting from the Reduction of Thick Cu_2O Films. *J. Am. Chem. Soc.* **2012**, *134*, 7231−7234.

(17) Li, C. W.; Ciston, J.; Kanan, M. W. Electroreduction of Carbon Monoxide to Liquid Fuel on Oxide-Derived Nanocrystalline Copper. *Nature* **2014**, *508*, 504−507.

(18) Rakhshani, A. E. Preparation, Characteristics and Photovoltaic Properties of Cuprous Oxide - a Review. *Solid-State Electron.* **1986**, *29*, 7−17.

(19) Hardee, K. L.; Bard, A. J. Semiconductor Electrodes X. Photoelectrochemical Behavior of Several Polycrystalline Metal Oxide Electrodes in Aqueous Solutions. *J. Electrochem. Soc.* **1977**, *124*, 215−224.

(20) Tennakone, K.; Jayatissa, A. H.; Punchihewa, S. Selective Photoreduction of Carbon Dioxide with Hydrous Cuprous Oxide. *J. Photochem. Photobiol., A* **1989**, *49*, 369−375.

(21) Filipič, G.; Cvelbar, U. Copper Oxide Nanowires: A Review of Growth. *Nanotechnology* **2012**, *23*, 194001.

(22) Wang, L. C.; de Tacconi, N. R.; Chenthamarakshan, C. R.; Rajeshwar, K.; Tao, M. Electrodeposited Copper Oxide Films: Effect of Bath pH on Grain Orientation and Orientation-Dependent Interfacial Behavior. *Thin Solid Films* **2007**, *515*, 3090−3095.

(23) Siegfried, M. J.; Choi, K. S. Elucidation of an Overpotential-Limited Branching Phenomenon Observed during the Electrocrystallization of Cuprous Oxide. *Angew. Chem., Int. Ed.* **2008**, *47*, 368−372.

(24) Kecsenovity, E.; Endrodi, B.; Pápa, Z.; Hernadi, K.; Rajeshwar, K.; Janaky, C. Ultralong Carbon Nanotubes Decorated with Cu_2O Nanocrystals: A Hybrid Platform for Enhanced Photoelectrochemical CO_2 Reduction. *J. Mater. Chem. A* **2016**, *4*, 3139−3147.

(25) Kuhl, K. P.; Cave, E. R.; Abram, D. N.; Jaramillo, T. F. New Insights into the Electrochemical Reduction of Carbon Dioxide on Metallic Copper Surfaces. *Energy Environ. Sci.* **2012**, *5*, 7050−7059.

(26) Ghadimkhani, G.; de Tacconi, N. R.; Chanmanee, W.; Janaky, C.; Rajeshwar, K. Efficient Solar Photoelectrosynthesis of Methanol from Carbon Dioxide Using Hybrid CuO-Cu_2O Semiconductor Nanorod Arrays. *Chem. Commun.* **2013**, *49*, 1297−1299.

(27) Rajeshwar, K.; de Tacconi, N. R.; Ghadimkhani, G.; Chanmanee, W.; Janáky, C. Tailoring Copper Oxide Semiconductor

DOI: 10.1021/acsenergylett.6b00078
ACS Energy Lett. XXXX, XXX, XXX−XXX

503 Nanorod Arrays for Photoelectrochemical Reduction of Carbon
504 Dioxide to Methanol. *ChemPhysChem* **2013**, *14*, 2251−2259.
505 (28) Homayoni, H.; Chanmanee, W.; de Tacconi, N. R.; Dennis, B.
506 H.; Rajeshwar, K. Continuous Flow Photoelectrochemical Reactor for
507 Solar Conversion of Carbon Dioxide to Alcohols. *J. Electrochem. Soc.*
508 **2015**, *162*, E115−E122.
509 (29) de Brito, J. F.; Araujo, A. R.; Rajeshwar, K.; Zanoni, M. V. B.
510 Photoelectrochemical Reduction of CO_2 on Cu/Cu_2O Films: Product
511 Distribution and pH Effects. *Chem. Eng. J.* **2015**, *264*, 302−309.
512 (30) Shi, C.; Hansen, H. A.; Lausche, A. C.; Nørskov, J. K. Trends in
513 Electrochemical CO_2 Reduction Activity for Open and Close-Packed
514 Metal Surfaces. *Phys. Chem. Chem. Phys.* **2014**, *16*, 4720−4727.
515 (31) Peterson, A. A.; Nørskov, J. K. Activity Descriptors for CO_2
516 Electroreduction to Methane on Transition-Metal Catalysts. *J. Phys.*
517 *Chem. Lett.* **2012**, *3*, 251−258.
518 (32) Lee, S.; Kim, D.; Lee, J. Electrocatalytic Production of C3-C4
519 Compounds by Conversion of CO_2 on a Chloride-Induced Bi-Phasic
520 Cu_2O-Cu Catalyst. *Angew. Chem.* **2015**, *127*, 14914−14918.
521 (33) Roberts, F. S.; Kuhl, K. P.; Nilsson, A. High Selectivity for
522 Ethylene from Carbon Dioxide Reduction over Copper Nanocube
523 Electrocatalysts. *Angew. Chem., Int. Ed.* **2015**, *54*, 5179−5182.
524 (34) Ren, D.; Wong, N. T.; Handoko, A. D.; Huang, Y.; Yeo, B. S.
525 Mechanistic Insights into the Enhanced Activity and Stability of
526 Agglomerated Cu Nanocrystals for the Electrochemical Reduction of
527 Carbon Dioxide to n-Propanol. *J. Phys. Chem. Lett.* **2016**, *7*, 20−24.
528 (35) Eilert, A.; Roberts, F. S.; Friebel, D.; Nilsson, A. Formation of
529 Copper Catalysts for CO_2 Reduction with High Ethylene/Methane
530 Product Ratio Investigated with In Situ X-Ray Absorption Spectros-
531 copy. *J. Phys. Chem. Lett.* **2016**, *7*, 1466−1470.
532 (36) Raciti, D.; Livi, K. J.; Wang, C. Highly Dense Cu Nanowires for
533 Low-Overpotential CO_2 Reduction. *Nano Lett.* **2015**, *15*, 6829−6835.
534 (37) Wang, Z.; Yang, G.; Zhang, Z.; Jin, M.; Yin, Y. Selectivity on
535 Etching: Creation of High-Energy Facets on Copper Nanocrystals for
536 CO_2 Electrochemical Reduction. *ACS Nano* **2016**, *10*, 4559−4564.
537 (38) Feng, X.; Jiang, K.; Fan, S.; Kanan, M. W. Grain-Boundary-
538 Dependent CO_2 Electroreduction Activity. *J. Am. Chem. Soc.* **2015**,
539 *137*, 4606−4609.
540 (39) Kas, R.; Hummadi, K. K.; Kortlever, R.; de Wit, P.; Milbrat, A.;
541 Luiten-Olieman, M. W. J.; Benes, N. E.; Koper, M. T. M.; Mul, G.
542 Three-Dimensional Porous Hollow Fibre Copper Electrodes for
543 Efficient and High-Rate Electrochemical Carbon Dioxide Reduction.
544 *Nat. Commun.* **2016**, *7*, 10748−10754.
545 (40) Chen, Y.; Li, C. W.; Kanan, M. W. Aqueous CO_2 Reduction at
546 Very Low Overpotential on Oxide-Derived Au Nanoparticles. *J. Am.*
547 *Chem. Soc.* **2012**, *134*, 19969−19972.
548 (41) Dutta, A.; Kuzume, A.; Rahaman, M.; Vesztergom, S.;
549 Broekmann, P. Monitoring the Chemical State of Catalysts for CO_2
550 Electroreduction: An In Operando Study. *ACS Catal.* **2015**, *5*, 7498−
551 7502.
552 (42) Gao, S.; Lin, Y.; Jiao, X.; Sun, Y.; Luo, Q.; Zhang, W.; Li, D.;
553 Yang, J.; Xie, Y. Partially Oxidized Atomic Cobalt Layers for Carbon
554 Dioxide Electroreduction to Liquid Fuel. *Nature* **2016**, *529*, 68−71.
555 (43) Gu, J.; Wuttig, A.; Krizan, J. W.; Hu, Y.; Detweiler, Z. M.; Cava,
556 R. J.; Bocarsly, A. B. Mg-Doped $CuFeO_2$ Photocathodes for
557 Photoelectrochemical Reduction of Carbon Dioxide. *J. Phys. Chem.*
558 *C* **2013**, *117*, 12415−12422.
559 (44) Kormányos, A.; Thomas, A.; Huda, M. N.; Sarker, P.; Liu, J. P.;
560 Poudyal, N.; Janáky, C.; Rajeshwar, K. Solution Combustion Synthesis,
561 Characterization, and Photoelectrochemistry of $CuNb_2O_6$ and
562 $ZnNb_2O_6$ Nanoparticles. *J. Phys. Chem. C* **2016**, DOI: 10.1021/
563 acs.jpcc.5b12738.

DOI: 10.1021/acsenergylett.6b00078
ACS Energy Lett. XXXX, XXX, XXX−XXX